

---

# Uncertainty Estimation with Infinitesimal Jackknife, Its Distribution and Mean-Field Approximation

---

**Zhiyun Lu**  
University of Southern California  
zhiyunlu@usc.edu

**Eugene Ie**  
Google Research  
eugeneie@google.com

**Fei Sha\***  
Google Research  
fsha@google.com

## Abstract

Uncertainty quantification is an important research area in machine learning. Many approaches have been developed to improve the representation of uncertainty in deep models to avoid overconfident predictions. Existing ones such as Bayesian neural networks and ensemble methods require modifications to the training procedures and are computationally costly for both training and inference. Motivated by this, we propose mean-field infinitesimal jackknife (mflJ) – a simple, efficient, and general-purpose plug-in estimator for uncertainty estimation. The main idea is to use infinitesimal jackknife, a classical tool from statistics for uncertainty estimation to construct a pseudo-ensemble that can be described with a closed-form Gaussian distribution, without retraining. We then use this Gaussian distribution for uncertainty estimation. While the standard way is to sample models from this distribution and combine each sample’s prediction, we develop a mean-field approximation to the inference where Gaussian random variables need to be integrated with the softmax nonlinear functions to generate probabilities for multinomial variables. The approach has many appealing properties: it functions as an ensemble without requiring multiple models, and it enables closed-form approximate inference using only the first and second moments of Gaussians. Empirically, mflJ performs competitively when compared to state-of-the-art methods, including deep ensembles, temperature scaling, dropout and Bayesian NNs, on important uncertainty tasks. It especially outperforms many methods on out-of-distribution detection.

## 1 Introduction

Recent advances in deep neural nets have dramatically improved predictive accuracy in supervised tasks. For many applications such as autonomous vehicle control and medical diagnosis, decision-making also needs accurate estimation of the uncertainty pertinent to the prediction. Unfortunately, deep neural nets are known to output overconfident, mis-calibrated predictions [19].

It is crucial to improve deep models’ ability in representing uncertainty. There have been a steady development of new methods on uncertainty quantification for deep neural nets. One popular idea is to introduce additional stochasticity (such as temperature annealing or dropout to network architecture) to existing trained models to represent uncertainty [16, 19]. Another line of work is to use an ensemble of models, collectively representing the uncertainty about the predictions. This ensemble of models can be obtained by varying training with respect to initialization [28], hyper-parameters [3], data partitions, *i.e.*, bootstraps [14, 42]. Yet another line of work is to use Bayesian neural networks (BNN), which can be seen as an ensemble of an infinite number of models, characterized by the posterior distribution [7, 32]. In practice, one samples models from the posterior or use variational inference. Each of those methods offers different trade-offs among computational costs, memory

---

\*On leave from the University of Southern California

consumptions, parallelization, and modeling flexibility. For example, while ensemble methods are often state-of-the-art, they are both computationally and memory intensive, for repeating training procedures or storing the resulting models.

Those stand in stark contrast to many practitioners’ desiderata. It would be the most ideal that neither training models nor inference with models incur additional memory and computational costs to estimate uncertainty beyond what is needed for making predictions. Additionally, it is also desirable to be able to quantify uncertainty on an existing model where re-training is not possible.

In this work, we propose a new method to bridge the gap. The main idea of our approach is to use Infinitesimal jackknife, a classical tool from statistics for uncertainty estimation [24], to construct a *pseudo-ensemble* that can be described with a closed-form Gaussian distribution. We then use this Gaussian distribution for uncertainty estimation. While the standard way is to sample models from this distribution and combine each sample’s prediction, we develop a mean-field approximation to the inference, where Gaussian random variables need to be integrated with the softmax nonlinear functions to generate probabilities for multinomial variables.

We show the proposed approach, which we refer to as mean-field Infinitesimal jackknife (mflJ) often surpasses or as competitive as existing approaches in evaluations metrics of NLL, ECE, and Out-of-Distribution detection accuracy on several benchmark datasets. mflJ shares appealing properties with several recent approaches for uncertainty estimation: constructing the pseudo-ensemble with infinitesimal jackknife does not require changing existing training procedures [42, 5, 17, 18, 25]; approximating the ensemble with a distribution removes the need of storing many models – an impractical task for modern learning models [10, 33]; the pseudo-ensemble distribution is in similar form as the Laplace approximation for Bayesian inference [4, 32] thus existing approaches in computational statistics such as Kronecker product factorization can be directly applied.

The mean-field approximation brings out an additional appeal. It is in closed-form and needs only the first and the second moments of the Gaussian random variables. In our case, the first moments are simply the predictions of the networks while the second moments involve the product between the inverse Hessian and a vector, which can be computed efficiently [1, 36, 40]. Additionally, the mean-field approximation can be applied when integrals in similar form need to be approximated. In Appendix B.3, we demonstrate its utility of applying it to the recently proposed SWAG algorithm for uncertainty estimation where the Gaussian distribution is derived differently [10, 23, 33, 35].

We describe our approach in §2, followed by a discussion on the related work in §3. Empirical studies are reported in §4, and we conclude in §5.

## 2 Approach

In this section, we start by introducing necessary notations and defining the task of uncertainty estimation. We then describe the technique of infinitesimal jackknife in §2.1. We derive a closed-form Gaussian distribution of an *infinite* number of models estimated with infinitesimal jackknife—we call them *pseudo-ensemble*. We describe how to use this distribution for uncertainty estimation in §2.2. We present our efficient mean-field approximation to Gaussian-softmax integral in §2.3. Lastly, we discuss hyper-parameters of our method and present the algorithm in §2.4.

**Notation** We are given a training set of  $N$  *i.i.d.* samples  $\mathcal{D} = \{z_i\}_{i=1}^N$ , where  $z_i = (x_i, y_i)$  with the input  $x_i \in \mathcal{X}$  and the target  $y_i \in \mathcal{Y}$ . We fit the data to a parametric predictive model  $y = f(x; \theta)$ . We define the loss on a sample  $z$  as  $\ell(z; \theta)$  and optimize the model’s parameter  $\theta$  via empirical risk minimization on  $\mathcal{D}$ . The minimizer is given by

$$\theta^* = \arg \min_{\theta} \mathcal{L}(\mathcal{D}; \theta), \text{ where } \mathcal{L}(\mathcal{D}; \theta) \stackrel{\text{def}}{=} \frac{1}{N} \sum_{i=1}^N \ell(z_i; \theta) \quad (1)$$

In practice, we are interested in not only the prediction  $f(x; \theta^*)$  but also quantifying the uncertainty of making such a prediction. In this paper, we consider (deep) neural network as the predictive model.

### 2.1 Infinitesimal jackknife and its distribution

Jackknife is a well-known resampling method to estimate the confidence interval of an estimator [44, 15]. It is a straightforward procedure. Each element  $z_i$  is left out from the dataset  $\mathcal{D}$  to form a unique

“leave-one-out” Jackknife sample  $\mathcal{D}_i = \mathcal{D} - \{z_i\}$ . A Jackknife sample’s estimate of  $\theta$  is given by

$$\hat{\theta}_i = \arg \min_{\theta} \mathcal{L}(\mathcal{D}_i; \theta) \quad (2)$$

We obtain  $N$  such samples  $\{\hat{\theta}_i\}_{i=1}^N$  and use them to estimate the variances of  $\theta^*$  and the predictions made with  $\theta^*$ . In this vein, this is a form of ensemble method.

However, it is not feasible to retrain modern neural networks  $N$  times, when  $N$  is often in the order of millions. Infinitesimal jackknife is a classical tool to approximate  $\hat{\theta}_i$  without re-training on  $\mathcal{D}_i$ . It is often used as a theoretical tool for asymptotic analysis [24], and is closely related to influence functions in robust statistics [11]. Recent studies have brought (renewed) interests in applying this methodology to machine learning problems [17, 25]. Here, we briefly summarize the method.

**Linear approximation.** The basic idea behind infinitesimal jackknife is to treat the  $\theta^*$  and  $\hat{\theta}_i$  as special cases of an estimator on weighted samples

$$\hat{\theta}(\mathbf{w}) = \arg \min_{\theta} \sum_i w_i \ell(z_i; \theta) \quad (3)$$

where the weights  $w_i$  form a  $(N - 1)$ -simplex:  $\sum_i w_i = 1$ . Thus the maximum likelihood estimate  $\theta^*$  is  $\hat{\theta}(\mathbf{w})$  when  $\mathbf{w} = \frac{1}{N}\mathbf{1}$ . A Jackknife sample’s estimate  $\hat{\theta}_i$ , on the other end, is  $\hat{\theta}(\mathbf{w})$  when  $\mathbf{w} = \frac{1}{N}(\mathbf{1} - \mathbf{e}_i)$  where  $\mathbf{e}_i$  is all-zero vector except taking a value of 1 at the  $i$ -th coordinate.

Using the first-order Taylor expansion around  $\mathbf{w} = \frac{1}{N}\mathbf{1}$ , we obtain (under the condition of twice-differentiability and the invertibility of the Hessian),

$$\hat{\theta}_i \approx \theta^* + \frac{1}{N} H^{-1}(\theta^*) \nabla \ell(z_i, \theta^*) \stackrel{\text{def}}{=} \theta^* + \frac{1}{N} H^{-1} \nabla_i \quad (4)$$

where  $H(\theta^*)$  is the Hessian matrix of  $\mathcal{L}$  evaluated at  $\theta^*$ , and  $\nabla \ell(z_i, \theta^*)$  is the gradient of  $\ell(z_i; \theta)$  evaluated at  $\theta^*$ . We use  $H$  and  $\nabla_i$  as shorthands when there is enough context to avoid confusion.

**An infinite number of infinitesimal jackknife samples.** If the number of samples  $N \rightarrow +\infty$ , we can characterize the “infinite” number of  $\hat{\theta}_i$  with a closed-form Gaussian distribution with the following sample mean and covariance as the distribution’s mean and covariance,

$$\begin{aligned} \hat{\theta}_i &\sim \mathcal{N}(\mathbf{m}, \Sigma_I), \quad \text{with } \mathbf{m} = \frac{1}{N} \sum_i \hat{\theta}_i = \theta^*, \text{ and} \\ \Sigma_I &= \frac{1}{N} \sum_i (\hat{\theta}_i - \theta^*)(\hat{\theta}_i - \theta^*)^\top = \frac{1}{N^2} H^{-1} \left[ \frac{1}{N} \sum_i \nabla_i \nabla_i^\top \right] H^{-1} = \frac{1}{N^2} H^{-1} J H^{-1} \end{aligned} \quad (5)$$

where  $J$  denotes the *observed* Fisher information matrix.

**Infinite infinitesimal bootstraps.** The above procedure and analysis can be extended to bootstrapping (*i.e.*, sampling with replacement). Similarly, to characterize the estimates from the bootstraps, we can also use a Gaussian distribution – details omitted here for brevity,

$$\hat{\theta}_i \sim \mathcal{N}(\theta^*, \Sigma_B), \quad \text{with } \Sigma_B = \frac{1}{N} H^{-1} J H^{-1}. \quad (6)$$

We refer to the distributions  $\mathcal{N}(\theta^*, \Sigma_I)$  and  $\mathcal{N}(\theta^*, \Sigma_B)$  as the *pseudo-ensemble distributions*. We can approximate further by  $H = J$  to obtain  $\Sigma_I \approx H^{-1}/N^2$  and  $\Sigma_B \approx H^{-1}/N$ .

Lakshminarayanan et al. [28] discussed that using models trained on bootstrapped samples does not work empirically as well as other approaches, as the learner only sees  $\sim 63\%$  of the dataset in each bootstrap sample. We note that this is an empirical limitation rather than a theoretical one. In practice, we can only train a very limited number of models. However, we hypothesize we can get the benefits of combining an *infinite* number of models *without* training. Empirical results valid this hypothesis.

## 2.2 Sampling based uncertainty estimation with the pseudo-ensemble distributions

Given the general form of the pseudo-ensemble distributions  $\theta \sim \mathcal{N}(\theta^*, \Sigma)$ , it is straightforward to see, if we approximate the predictive function  $f(\cdot, \cdot)$  with a linear function,

$$f(x; \theta) \approx f(x; \theta^*) + \nabla f^\top (\theta - \theta^*),$$

we can then regard the predictions by the models as a Gaussian distributed random variable,

$$f(x; \theta) \sim \mathcal{N}(f(x; \theta^*), \nabla f^\top \Sigma \nabla f).$$

For predictive functions whose outputs are approximately Gaussian, it might be adequate to characterize the uncertainty with the approximated mean and variance. However, for predictive functions that are categorical, this approach is not applicable.

A standard way is to use the sampling for combining the discrete predictions from the models in the ensemble. For example, for classification  $y = \arg \max_c f_c(x; \theta)$  where  $f_c$  is the probability of labeling  $x$  with  $c$ -th category, the averaged prediction from the ensemble is then

$$e_k = \mathbb{E}[P(y = k)] \approx \frac{1}{M} \sum_{i=1}^M \mathbb{1}[\arg \max_c f_c(x; \theta_i) = k] \quad (7)$$

where  $\theta_i \sim \mathcal{N}(\theta^*, \Sigma)$ , and  $\mathbb{1}$  is the indicator function. In the next section, we propose a new approach that avoids sampling and directly approximates the ensemble prediction of discrete labels.

### 2.3 Mean-field approximation for Gaussian-softmax integration

In deep neural network for classification, the predictions  $f_k(\cdot)$  are the outputs of the softmax layer.

$$f_k = \text{SOFTMAX}(a_k) \propto \exp\{a_k\}, \text{ with } \mathbf{a} = \mathbf{g}(x; \phi)^\top \mathbf{W}, \quad (8)$$

where  $\mathbf{g}(x; \phi)$  is the transformation of the input through the layers before the fully-connected layer, and  $\mathbf{W}$  is the connection weights in the softmax layer. We focus on the case  $\mathbf{g}(x; \phi)$  is deterministic – extending to the random variables is straightforward. As discussed, we assume the pseudo-ensemble on  $\mathbf{W}$  forms a Gaussian distribution  $\mathbf{W} \sim \mathcal{N}(\mathbf{W}^*; \Sigma)$ . Then we have  $\mathbf{a} \sim \mathcal{N}(\boldsymbol{\mu}, \mathbf{S})$  such that

$$\boldsymbol{\mu} = \mathbf{g}(x; \phi)^\top \mathbf{W}^*, \quad \mathbf{S} = \mathbf{g}(x; \phi)^\top \Sigma \mathbf{g}(x; \phi)^2. \quad (9)$$

We give detailed derivation in Appendix A to compute the expectation of  $f_k$ ,

$$e_k = \mathbb{E}[f_k] = \int \text{SOFTMAX}(a_k) \mathcal{N}(\mathbf{a}; \boldsymbol{\mu}, \mathbf{S}) d\mathbf{a} \quad (10)$$

The key idea is to apply the mean-field approximation  $\mathbb{E}[f(x)] \approx f(\mathbb{E}[x])$  and use the following well-known formula to compute the Gaussian integral of a sigmoid function  $\sigma(\cdot)$ ,

$$\int \sigma(a) \mathcal{N}(a; \mu, s^2) \approx \sigma\left(\frac{\mu}{\sqrt{1 + \lambda_0 s^2}}\right)$$

where  $\lambda_0$  is a constant and is usually chosen to be  $\pi/8$  or  $3/\pi^2$ . In the softmax case, we arrive at:

$$\text{Mean-Field 0 (mf0)} \quad e_k \approx \left( \sum_i \exp\left(-\frac{(\mu_k - \mu_i)}{\sqrt{1 + \lambda_0 s_k^2}}\right) \right)^{-1} \quad (11)$$

$$\text{Mean-Field 1 (mf1)} \quad e_k \approx \left( \sum_i \exp\left(-\frac{(\mu_k - \mu_i)}{\sqrt{1 + \lambda_0 (s_k^2 + s_i^2)}}\right) \right)^{-1} \quad (12)$$

$$\text{Mean-Field 2 (mf2)} \quad e_k \approx \left( \sum_i \exp\left(-\frac{(\mu_k - \mu_i)}{\sqrt{1 + \lambda_0 (s_k^2 + s_i^2 - 2s_{ik})}}\right) \right)^{-1} \quad (13)$$

The 3 approximations differ in how much information from  $i \neq k$  is considered: not considering  $s_i$ , considering its variance  $s_i^2$  and considering its covariance  $s_{ik}$ . Note that mf0 and mf1 are computationally preferred over mf2 which uses  $K^2$  covariances, where  $K$  is the number of classes. ([12] derived an approximation in the form of mf2 but did not apply to uncertainty estimation.)

---

<sup>2</sup>With slight abuse of notation, the form of  $\mathbf{S}$  is after proper vectorization and padding of  $\mathbf{g}$  and  $\Sigma$ .

**Intuition** The simple form of the mean-field approximations makes it possible to understand them intuitively. We focus on mf0. We first rewrite it in the familiar “softmax” form:

$$(mf0) \quad e_k \approx \frac{e^{\frac{\mu_k}{\sqrt{1+\lambda_0 s_k^2}}}}{\sum_i e^{\frac{\mu_i}{\sqrt{1+\lambda_0 s_k^2}}}} \stackrel{\text{def}}{=} \hat{e}_k.$$

Note that this form is similar to a “softmax” with a temperature scaling:  $P(y = k) \propto \exp\left\{\frac{\mu_k}{T}\right\}$ . However, there are several important differences. In mf0, the temperature scaling factor is category-specific:

$$\hat{e}_k \propto \exp\left\{\frac{\mu_k}{T_k}\right\} \quad \text{with} \quad T_k = \sqrt{1 + \lambda_0 s_k^2}. \quad (14)$$

Importantly, the factor  $T_k$  depends on the variance of the category. For a prediction with high variance, the temperature for that category is high, reducing the corresponding “probability”  $\hat{e}_k$ . Specifically,

$$\hat{e}_k \rightarrow \frac{1}{K} \quad \text{as} \quad s_k \rightarrow +\infty.$$

In other words, the scaling factor is both *category-specific* and *data-dependent*, providing additional flexibility to a global temperature scaling factor.

**Implementation nuances** Because of this category-specific temperature scaling,  $\hat{e}_k$  (and approximations from mf1 and mf2) is no longer a multinomial probability. Proper normalization should be performed,  $e_k \approx \frac{\hat{e}_k}{\sum_i \hat{e}_i} \stackrel{\text{def}}{=} p_k$ .

## 2.4 Other implementation considerations

**Temperature scaling.** Temperature scaling was shown to be useful for obtaining calibrated probabilities [19]. This can be easily included as well with

$$f_k \propto \exp(T_{\text{act}}^{-1} a_k) \quad (15)$$

We can also combine with another “temperature” scaling factor, representing how well the models in the pseudo-ensemble are concentrated

$$\theta \sim \mathcal{N}(\theta^*, T_{\text{ens}}^{-1} \Sigma) \quad (16)$$

Here  $T_{\text{ens}}$  is for the pseudo-ensembles or the posterior [46]. Note that these two temperatures control variability differently. When  $T_{\text{ens}} \rightarrow 0$ , the ensemble focuses on one model. When  $T_{\text{act}} \rightarrow 0$ , each model in the ensemble moves to “hard” decisions, as in eq. (7). Using mf0 as an example,

$$e_k = \left( \sum_i \exp\left(-(\mu_k - \mu_i) (T_{\text{act}}^2 + \lambda_0 s_k^2 / T_{\text{ens}})^{-\frac{1}{2}}\right) \right)^{-1} \quad (17)$$

where  $s_k$  is computed at  $T_{\text{ens}} = 1$ . Empirically, we can tune the temperatures  $T_{\text{ens}}$  and  $T_{\text{act}}$  as hyper-parameters on a heldout set, to optimize the predictive performance.

**Computation complexity and scalability.** The bulk of the computation, as in Bayesian approximate inference, lies in the computation of  $H^{-1}$  in  $\Sigma_I$  and  $\Sigma_B$ , as in eq. (5) and eq. (6), or more precisely the product between the inverse Hessian and vectors, cf. eq. (9). For smaller models, computing and storing  $H^{-1}$  exactly is attractive. For large models, one can compute the inverse Hessian-vector product approximately using multiple Hessian-vector products [40, 1, 25]. Alternatively, we can approximate inverse Hessian using Kronecker factorization [41]. In short, any advances in computing the inverse Hessian and related quantities can be used to accelerate computation needed in this paper.

**An application example.** In Algorithm 1, we exemplify the application of the mean-field approximation to Gaussian-softmax integration in the uncertainty estimation. For brevity, we consider the last-layer/fully-connected layer’s parameters  $\mathbf{W}$  as a part of the deep neural network’s parameters  $\theta = (\phi, \mathbf{W})$ . We assume the mapping  $g(x; \phi)$  prior to the fully connected layer is deterministic.

---

**Algorithm 1:** Uncertainty estimate with Mean-Field Infinitesimal jackknife (mflJ)

---

- 1 **Input:** A deep neural net model  $\theta^* = (\phi^*, \mathbf{W}^*)$ , a training set  $\mathcal{D}$ ,  $T_{\text{ens}}$ ,  $T_{\text{act}}$ , and a test point  $x$ .
  - 2 Compute pre-fully-connected layer features  $g(x; \phi^*)$
  - 3 Compute the moments  $\boldsymbol{\mu}$ ,  $\mathbf{S}$  of the logits via eq. (9), using either of the following two approaches
  - 4     Compute  $H^{-1}(\mathbf{W}^*)$  on  $\mathcal{D}$  and the inverse Hessian-vector product exactly  $H^{-1}(\mathbf{W}^*)\mathbf{v}$
  - 5     Compute the inverse Hessian-vector product approximately [1]
  - 6 Compute  $e_k$  via mean-field approximation eq. (11), (12) or (13), and normalize  $e_k$  to obtain  $p_k$ .
  - 7 **Output:** The predictive uncertainty is  $p_k$ .
- 

### 3 Related Work

Resampling methods, such as jackknife and bootstrap, are classical statistical tools for assessing confidence intervals [44, 37, 15, 14]. Recent results have shown that carefully designed jackknife estimators [5] can achieve worst-case coverage guarantees on regression problems.

However, the exhaustive re-training in jackknife or bootstrap can be cumbersome in practice. Recent works have leveraged the idea of influence function [25, 11] to alleviate the computational challenge. [42] combines the influence function with random data weight samples to approximate the variance of predictions in bootstrapping; [2] derives higher-order influence function approximation for Jackknife estimators. Theoretical properties of the approximation are studied in [17, 18]. [34] applies this approximation to identify underdetermined test points. Infinitesimal jackknife follows the same idea as those work [24, 17, 18]. To avoid explicitly storing those models, we seek a Gaussian distribution to approximately characterize the model. This connects to several existing research.

The posterior of a Bayesian model can be approximated with a Gaussian distribution [32, 41]:  $\theta \sim \mathcal{N}(\theta^*, H^{-1})$ , where  $\theta^*$  is interpreted as the maximum a posterior estimate (thus incorporating any prior the model might want to include). If we approximate the observed Fisher information matrix  $J$  in eq. (5) with the Hessian  $H$ , the two pseudo-ensemble distributions and the Laplace approximation to the posterior have identical forms except that the Hessians are scaled differently, and can be captured by the ensemble temperature eq. (16). Note that despite the similarity, infinitesimal jackknife are “frequentist” methods and do not assume well-formed Bayesian modeling.

The trajectory of stochastic gradient descent gives rise to a sequence of models where the covariance matrix among batch means converges to  $H^{-1}JH^{-1}$  [9, 10, 33], similar to the pseudo-ensemble distributions in form. But note that those approaches do not collect information around the maximum likelihood estimate, while we do. It is also a classical result that the maximum likelihood estimator converges in distribution to a normal distribution.  $\theta^*$  and  $\frac{1}{N}H^{-1}$  are simply the plug-in estimators of the truth mean and the covariance of this asymptotic distribution.

### 4 Experiments

We first describe the setup for our empirical studies. We then demonstrate the effectiveness of the proposed approach on the MNIST dataset, mainly contrasting the results from sampling to those from mean-field approximation and other implementation choices. We then provide a detailed comparison to popular approaches for uncertainty estimation. In the main text, we focus on classification problems. We evaluate on commonly used benchmark datasets, summarized in Table 1. In Appendix B.5, we report results on regression tasks.

#### 4.1 Setup

**Model and training details for classifiers.** For MNIST, we train a two-layer MLP with 256 ReLU units per layer, using Adam optimizer for 100 epochs. For CIFAR-10, we train a ResNet-20 with Adam for 200 epochs. On CIFAR-100, we train a DenseNet-BC-121 with SGD optimizer for 300 epochs. For ILSVRC-2012, we train a ResNet-50 with SGD optimizer for 90 epochs.

**Evaluation tasks and metrics.** We evaluate on two tasks: predictive uncertainty on in-domain samples, and detection of out-of-distribution samples. For in-domain predictive uncertainty, we report classification error rate ( $\varepsilon$ ), negative log-likelihood (NLL), and expected calibration error

Table 1: Datasets for Classification Tasks and Out-of-Distribution (OOD) Detection

Dataset Name	# of classes	train, held-out and test splits	OOD Dataset	held-out and test splits
MNIST [29]	10	55k / 5k / 10k	NotMNIST [8]	5k / 13.7k
CIFAR-10 [27]	10	45k / 5k / 10k	LSUN (resized) [47]	1k / 9k
CIFAR-100 [27]	100		SVHN [39]	5k / 21k
ILSVRC-2012 [13]	1,000	1,281k / 25k / 25k	Imagenet-O [21]	2k / - <sup>†</sup>

<sup>†</sup>: the number of samples is limited; best results on held-out are reported.

in  $\ell_1$  distance (ECE) [19] on the test set. NLL is a proper scoring rule [28], and measures the KL-divergence between the ground-truth data distribution and the predictive distribution of the classifiers. ECE measures the discrepancy between the histogram of the predicted probabilities by the classifiers and the observed ones in the data – properly calibrated classifiers will yield matching histograms. Both metrics are commonly used in the literature and the lower the better. In Appendix B.1, we give precise definitions.

On the task of out-of-distribution (OOD) detection, we assess how well  $p(x)$ , the classifier’s output being interpreted as probability, can be used to distinguish invalid samples from normal in-domain images. Following the common practice [20, 31, 30], we report two threshold-independent metrics: area under the receiver operating characteristic curve (AUROC), and area under the precision-recall curve (AUPR). Since the precision-recall curve is sensitive to the choice of positive class, we report both “AUPR in:out” where in-distribution and out-of-distribution images are specified as positives respectively. We also report detection accuracy, the optimal accuracy achieved among all thresholds in classifying in-/out-domain samples. All three metrics are the higher the better.

**Competing approaches for uncertainty estimation.** We compare to popular approaches: (i) frequentist approaches: the point estimator of maximum likelihood estimator (MLE) as a baseline, the temperature scaling calibration (T. SCALE) [19], the deep ensemble method (ENSEMBLE) [28], and the resampling bootstrap RUE [42]. (ii) variants of Bayesian neural networks (BNN): DROPOUT [16] approximates the Bayesian posterior using stochastic forward passes of the network with dropout. BNN(VI) trains the network via stochastic variational inference to maximize the evidence lower bound. BNN(KFAC) applies the Laplace approximation to construct a Gaussian posterior, via layer-wise Kronecker product factorized covariance matrices [41].

**Hyper-parameter tuning.** For in-domain uncertainty estimation, we use the NLL on the held-out sets to tune hyper-parameters. For the OOD detection task, we use AUROC on the held-out to select hyper-parameters. We report the results of the best hyper-parameters on the test sets. The key hyper-parameters are the temperatures, regularization or prior in BNN methods, and dropout rates.

**Other implementation details.** When Hessian needs to be inverted, we add a dampening term  $\tilde{H} = (H + \epsilon I)$  following [41, 42] to ensure positive semi-definiteness and the smallest eigenvalue of  $\tilde{H}$  be 1. For BNN(VI), we use Flipout [45] to reduce gradient variances and follow [43] for variational inference on deep ResNets. On ImageNet, we compute the Kronecker-product factorized Hessian matrix, rather than full due to high dimensionality. For BNN(KFAC) and RUE, we use mini-batch approximations on subsets of the training set to scale up on ImageNet, as suggested in [41, 42].

## 4.2 Infinitesimal jackknife on MNIST

Most uncertainty quantification methods, including the ones proposed in this paper, have “knobs” to tune. We first concentrate on MNIST and perform extensive studies of the proposed approaches to understand several design choices. Table 2 contrasts them.

**Use all layers or just the last layer.** Uncertainty quantification on deep neural nets is computationally costly, given their large number of parameters, especially when the methods need information on the curvatures of the loss functions. To this end, many approaches assume layer-wise independence [41] and low-rank components [33, 38] and in some cases, restrict uncertainty quantification to only a few layers [48] – in particular, the last layer [26]. The top portion of Table 2 shows the restricting to the last layer harms the in-domain ECE slightly but improves OOD significantly.

Table 2: Performance of Infinitesimal jackknife Pseudo-Ensemble Distribution on MNIST

which layer(s)	approx. method	MNIST: in-domain ( $\downarrow$ )	NotMNIST: OOD detection ( $\uparrow$ )					
			$\varepsilon$ (%)	NLL	ECE (%)	Acc. (%)	AU ROC	AU PR (in : out)
all	500	<b>1.66</b>	0.06	0.42	87.46	92.50	87.01 : 93.52	
last	sampling (§2.2)	20	1.74	0.06	0.41	87.58	93.48	91.66 : 94.27
last	$M =$	100	1.68	0.05	0.47	90.10	95.55	94.62 : 96.08
last		500	1.67	0.05	0.50	90.77	96.20	95.79 : 96.47
last	mean-field	mf0	1.67	<b>0.05</b>	<b>0.20</b>	<b>91.93</b>	96.91	96.67 : 96.99
last	( $M = 0$ )	mf1	1.67	0.05	0.47	91.91	96.93	96.72 : 97.03
last		mf2	1.67	0.05	0.46	91.91	<b>96.94</b>	<b>96.72 : 97.03</b>

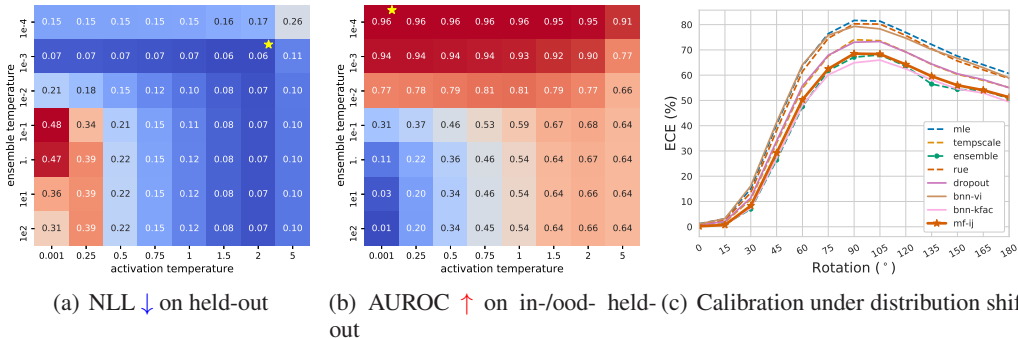


Figure 1: Best viewed in colors. (a-b) Effects of the softmax and ensemble temperatures on NLL and AUROC. The yellow star marks the best pairs of temperatures. See texts for details.

**Effectiveness of mean-field approximation.** Table 2 also shows that the mean-field approximation has similar performance as sampling (the distribution) on the in-domain tasks but noticeably improves on OOD detection. mf0 performs the best among the 3 variants.

**Effect of ensemble and activation temperatures.** We study the roles of ensemble and activation temperatures in mflJ (§2.4). We grid search the two and generate the heatmaps of NLL and AU ROC on the held-out sets, shown in Figure 1. Note that ( $T_{ens} = 0, T_{act} = 1$ ) correspond to MLE.

What is particularly interesting is that for NLL, higher activation temperature ( $T_{act} \geq 1$ ) and lower ensemble temperature ( $T_{ens} \leq 10^{-2}$ ) work the best. For AU ROC, however, lower temperatures on both work best. That lower  $T_{ens}$  is preferred was also observed in [46] and using  $T_{act} > 1$  for better calibration is noted in [19]. On the other end, for OOD detection, [31] suggests a very high activation temperature ( $T_{act} = 1000$  in their work, likely due to using a single model instead of an ensemble).

### 4.3 Comparison to other approaches

Given our results in the previous section, we report mf0 of infinitesimal jackknife in the rest of the paper. Table 3 contrasts various methods on in-domain tasks of MNIST, CIFAR-100, and ImageNet. Table 4 contrasts performances on the out-of-distribution detection task (OOD). Results on CIFAR-10 (both in-domain and OOD), as well as CIFAR-100 OOD on SVNH are in Appendix B.4.

While deep ensemble [28] achieves the best performance on in-domain tasks most of time, the proposed approach mflJ typically outperforms other approaches, especially on the calibration metric ECE. On the OOD detection task, mflJ significantly outperforms all other approaches in all metrics.

ImageNet-O is a particularly hard dataset for OOD [21]. The images are from ImageNet-22K samples, thus share similar low-level statistics as the in-domain data. Moreover, the images are chosen such that they are misclassified by existing networks (ResNet-50) with high confidence, or so called “natural adversarial examples”. We follow [21] to use 200-class subset, which are the confusing classes to the OOD images, of the test set as the in-distribution examples. [21] further demonstrates that many popular approaches to improve neural network robustness, like adversarial training, hardly help on ImageNet-O. mflJ improves over other baselines by a margin.



Table 3: Comparing different uncertainty estimate methods on in-domain tasks (lower is better)

Method	MNIST			CIFAR-100			ImageNet		
	$\epsilon$ (%)	NLL	ECE (%)	$\epsilon$ (%)	NLL	ECE (%)	$\epsilon$ (%)	NLL	ECE (%)
MLE	1.67	0.10	1.18	24.3	1.03	10.4	23.66	0.92	3.03
T. SCALE	1.67	0.06	0.74	24.3	0.92	3.13	23.66	0.92	2.09
ENSEMBLE	<b>1.25</b>	<b>0.05</b>	0.30	<b>19.6</b>	<b>0.71</b>	2.00	<b>21.22</b>	<b>0.83</b>	3.10
RUE #	1.72	0.08	0.85	24.3	0.99	8.60	23.63	0.92	2.83
DROPOUT	1.67	0.06	0.68	23.7	0.84	3.43	24.93	0.99	1.62
BNN(VI) #	1.72	0.14	1.13	25.6	0.98	8.35	26.54	1.17	4.41
BNN(KFAC)	1.71	0.06	<b>0.16</b>	24.1	0.89	3.36	23.64	0.92	2.95
mflJ	1.67	<b>0.05</b>	0.20	24.3	0.91	<b>1.49</b>	23.66	0.91	<b>0.93</b>

#: for CIFAR-100 and ImageNet, only the last layer is used due to the high computational cost.

Table 4: Comparing different methods on out-of-distribution detection (higher is better)

Method	MNIST vs. NotMNIST			CIFAR-100 vs. LSUN			ImageNet vs. ImageNet-O		
	Acc. <sup>†</sup>	ROC <sup>‡</sup>	PR <sup>§</sup>	Acc. <sup>†</sup>	ROC <sup>‡</sup>	PR <sup>§</sup>	Acc. <sup>†</sup>	ROC <sup>‡</sup>	PR <sup>§</sup>
MLE	67.6	53.8	40.1 : 72.5	72.7	80.0	83.5 : 75.2	58.4	51.6	78.4 : 26.3
T. SCALE	67.4	66.7	48.8 : 77.0	76.6	84.3	86.7 : 80.3	58.5	54.5	79.2 : 27.8
ENSEMBLE	86.5	88.0	70.4 : 92.8	74.4	82.3	85.7 : 77.8	60.1	50.6	78.9 : 25.7
RUE	61.1	64.7	60.5 : 68.4	75.2	83.0	86.7 : 77.8	58.4	51.6	78.3 : 26.3
DROPOUT	88.8	91.4	78.7 : 93.5	69.8	77.3	81.1 : 72.9	59.5	51.7	79.0 : 26.3
BNN(VI) #	86.9	81.1	59.8 : 89.9	62.5	67.7	71.4 : 63.1	57.8	52.0	75.7 : 26.8
BNN(KFAC)	88.7	93.5	89.1 : 93.8	72.9	80.4	83.9 : 75.5	60.3	53.1	79.6 : 26.9
mflJ	<b>91.9</b>	<b>96.9</b>	<b>96.7 : 97.0</b>	<b>82.2</b>	<b>89.9</b>	<b>92.0 : 86.6</b>	<b>63.2</b>	<b>62.9</b>	<b>83.5 : 33.3</b>

<sup>†</sup>: Accuracy (%). <sup>‡</sup>: Area under ROC. <sup>§</sup>: Area under Precision-Recall with “in” vs. “out” domains flipped.

#: for CIFAR-100 and ImageNet, only the last layer is used for due to the high computational cost.

**Robustness to distributional shift.** [43] points out that many uncertainty estimation methods are sensitive to distributional shift. Thus, we evaluate the robustness of mflJ on rotated MNIST images, from 0 to 180°. The ECE curves in Figure 1(c) show mflJ is better or as robust as other approaches.

## 5 Conclusion

We propose a simple, efficient, and general-purpose confidence estimator mflJ for deep neural networks. The main idea is to approximate the ensemble of an infinite number of infinitesimal jackknife samples with a closed-form Gaussian distribution, and derive an efficient mean-field approximation to classification predictions, when the softmax layer is applied to Gaussian. Empirically, mflJ surpasses or is competitive with the state-of-the-art methods for uncertainty estimation while incurring lower computational cost and memory footprint.

## References

- [1] Naman Agarwal, Brian Bullins, and Elad Hazan. Second-order stochastic optimization in linear time. *stat*, 1050:15, 2016.
- [2] Ahmed M. Alaa and Mihaela van der Schaar. *The Discriminative Jackknife: Quantifying Predictive Uncertainty via Higher-order Influence Functions*, 2019. URL <https://openreview.net/forum?id=H1xauR4Kvr>.
- [3] Arsenii Ashukha, Alexander Lyzhov, Dmitry Molchanov, and Dmitry Vetrov. Pitfalls of in-domain uncertainty estimation and ensembling in deep learning. *arXiv preprint arXiv:2002.06470*, 2020.
- [4] David Barber and Christopher M Bishop. Ensemble learning for multi-layer networks. In *Advances in neural information processing systems*, pages 395–401, 1998.
- [5] Rina Foygel Barber, Emmanuel J Candes, Aaditya Ramdas, and Ryan J Tibshirani. Predictive inference with the jackknife+. *arXiv preprint arXiv:1905.02928*, 2019.

- [6] Christopher M. Bishop. *Pattern Recognition and Machine Learning*. Springer, 2006.
- [7] Charles Blundell, Julien Cornebise, Koray Kavukcuoglu, and Daan Wierstra. Weight uncertainty in neural networks. *arXiv preprint arXiv:1505.05424*, 2015.
- [8] Yaroslav Bulatov. Notmnist dataset. *Google (Books/OCR), Tech. Rep.[Online]. Available: <http://yaroslavvb.blogspot.it/2011/09/notmnist-dataset.html>*, 2, 2011.
- [9] Tianqi Chen, Emily Fox, and Carlos Guestrin. Stochastic gradient hamiltonian monte carlo. In *International conference on machine learning*, pages 1683–1691, 2014.
- [10] Xi Chen, Jason D Lee, Xin T Tong, and Yichen Zhang. Statistical inference for model parameters in stochastic gradient descent. *arXiv preprint arXiv:1610.08637*, 2016.
- [11] R Dennis Cook and Sanford Weisberg. *Residuals and influence in regression*. New York: Chapman and Hall, 1982.
- [12] Jean Daunizeau. Semi-analytical approximations to statistical moments of sigmoid and softmax mappings of normal variables. *arXiv preprint arXiv:1703.00091*, 2017.
- [13] Jia Deng, Wei Dong, Richard Socher, Li-Jia Li, Kai Li, and Li Fei-Fei. Imagenet: A large-scale hierarchical image database. In *2009 IEEE conference on computer vision and pattern recognition*, pages 248–255. Ieee, 2009.
- [14] Bradley Efron. Bootstrap methods: another look at the jackknife. In *Breakthroughs in statistics*, pages 569–593. Springer, 1992.
- [15] Bradley Efron and Charles Stein. The jackknife estimate of variance. *The Annals of Statistics*, pages 586–596, 1981.
- [16] Yarín Gal and Zoubin Ghahramani. Dropout as a bayesian approximation: Representing model uncertainty in deep learning. In *international conference on machine learning*, pages 1050–1059, 2016.
- [17] Ryan Giordano, Will Stephenson, Runjing Liu, Michael I Jordan, and Tamara Broderick. A swiss army infinitesimal jackknife. *arXiv preprint arXiv:1806.00550*, 2018.
- [18] Ryan Giordano, Michael I Jordan, and Tamara Broderick. A higher-order swiss army infinitesimal jackknife. *arXiv preprint arXiv:1907.12116*, 2019.
- [19] Chuan Guo, Geoff Pleiss, Yu Sun, and Kilian Q Weinberger. On calibration of modern neural networks. *arXiv preprint arXiv:1706.04599*, 2017.
- [20] Dan Hendrycks and Kevin Gimpel. A baseline for detecting misclassified and out-of-distribution examples in neural networks. *arXiv preprint arXiv:1610.02136*, 2016.
- [21] Dan Hendrycks, Kevin Zhao, Steven Basart, Jacob Steinhardt, and Dawn Song. Natural adversarial examples. *arXiv preprint arXiv:1907.07174*, 2019.
- [22] José Miguel Hernández-Lobato and Ryan Adams. Probabilistic backpropagation for scalable learning of bayesian neural networks. In *International Conference on Machine Learning*, pages 1861–1869, 2015.
- [23] Pavel Izmailov, Dmitrii Podoprikin, Timur Garipov, Dmitry Vetrov, and Andrew Gordon Wilson. Averaging weights leads to wider optima and better generalization. *arXiv preprint arXiv:1803.05407*, 2018.
- [24] Louis A Jaekel. *The infinitesimal jackknife*. Bell Telephone Laboratories, 1972.
- [25] Pang Wei Koh and Percy Liang. Understanding black-box predictions via influence functions. In *Proceedings of the 34th International Conference on Machine Learning-Volume 70*, pages 1885–1894. JMLR. org, 2017.
- [26] Agustinus Kristiadi, Matthias Hein, and Philipp Hennig. Being bayesian, even just a bit, fixes overconfidence in relu networks. *arXiv preprint arXiv:2002.10118*, 2020.

- [27] A Krizhevsky. Learning multiple layers of features from tiny images. *Master's thesis, University of Tront*, 2009.
- [28] Balaji Lakshminarayanan, Alexander Pritzel, and Charles Blundell. Simple and scalable predictive uncertainty estimation using deep ensembles. In *Advances in Neural Information Processing Systems*, pages 6405–6416, 2017.
- [29] Yann LeCun, Corinna Cortes, and Christopher JC Burges. The mnist database of handwritten digits, 1998. URL <http://yann.lecun.com/exdb/mnist>, 10:34, 1998.
- [30] Kimin Lee, Kibok Lee, Honglak Lee, and Jinwoo Shin. A simple unified framework for detecting out-of-distribution samples and adversarial attacks. In *Advances in Neural Information Processing Systems*, pages 7165–7175, 2018.
- [31] Shiyu Liang, Yixuan Li, and R Srikant. Enhancing the reliability of out-of-distribution image detection in neural networks. *arXiv preprint arXiv:1706.02690*, 2017.
- [32] David JC MacKay. *Bayesian methods for adaptive models*. PhD thesis, California Institute of Technology, 1992.
- [33] Wesley J Maddox, Pavel Izmailov, Timur Garipov, Dmitry P Vetrov, and Andrew Gordon Wilson. A simple baseline for bayesian uncertainty in deep learning. In *Advances in Neural Information Processing Systems*, pages 13132–13143, 2019.
- [34] David Madras, James Atwood, and Alex D'Amour. Detecting extrapolation with local ensembles. *arXiv preprint arXiv:1910.09573*, 2019.
- [35] Stephan Mandt, Matthew D Hoffman, and David M Blei. Stochastic gradient descent as approximate bayesian inference. *The Journal of Machine Learning Research*, 18(1):4873–4907, 2017.
- [36] James Martens. Deep learning via hessian-free optimization. In *ICML*, volume 27, pages 735–742, 2010.
- [37] Rupert G Miller. The jackknife-a review. *Biometrika*, 61(1):1–15, 1974.
- [38] Aaron Mishkin, Frederik Kunstner, Didrik Nielsen, Mark Schmidt, and Mohammad Emtiyaz Khan. Slang: Fast structured covariance approximations for bayesian deep learning with natural gradient. In *Advances in Neural Information Processing Systems*, pages 6245–6255, 2018.
- [39] Yuval Netzer, Tao Wang, Adam Coates, Alessandro Bissacco, Bo Wu, and Andrew Ng. Reading digits in natural images with unsupervised feature learning. *NIPS*, 01 2011.
- [40] Barak A Pearlmutter. Fast exact multiplication by the hessian. *Neural computation*, 6(1): 147–160, 1994.
- [41] Hippolyt Ritter, Aleksandar Botev, and David Barber. A scalable laplace approximation for neural networks. In *6th International Conference on Learning Representations, ICLR 2018-Conference Track Proceedings*, volume 6. International Conference on Representation Learning, 2018.
- [42] Peter Schulam and Suchi Saria. Can you trust this prediction? auditing pointwise reliability after learning. *arXiv preprint arXiv:1901.00403*, 2019.
- [43] Jasper Snoek, Yaniv Ovadia, Emily Fertig, Balaji Lakshminarayanan, Sebastian Nowozin, D Sculley, Joshua Dillon, Jie Ren, and Zachary Nado. Can you trust your model's uncertainty? evaluating predictive uncertainty under dataset shift. In *Advances in Neural Information Processing Systems*, pages 13969–13980, 2019.
- [44] John Tukey. Bias and confidence in not quite large samples. *Ann. Math. Statist.*, 29:614, 1958.
- [45] Yeming Wen, Paul Vicol, Jimmy Ba, Dustin Tran, and Roger Grosse. Flipout: Efficient pseudo-independent weight perturbations on mini-batches. *arXiv preprint arXiv:1803.04386*, 2018.

- [46] Florian Wenzel, Kevin Roth, Bastiaan S Veeling, Jakub Światkowski, Linh Tran, Stephan Mandt, Jasper Snoek, Tim Salimans, Rodolphe Jenatton, and Sebastian Nowozin. How good is the bayes posterior in deep neural networks really? *arXiv preprint arXiv:2002.02405*, 2020.
- [47] Fisher Yu, Ari Seff, Yinda Zhang, Shuran Song, Thomas Funkhouser, and Jianxiong Xiao. Lsun: Construction of a large-scale image dataset using deep learning with humans in the loop. *arXiv preprint arXiv:1506.03365*, 2015.
- [48] Jiaming Zeng, Adam Lesnikowski, and Jose M Alvarez. The relevance of bayesian layer positioning to model uncertainty in deep bayesian active learning. *arXiv preprint arXiv:1811.12535*, 2018.

## A Mean-Field Approximation for Gaussian-softmax Integration

In this section, we derive the mean-field approximation for Gaussian-softmax integration, eq. (10) in the main text. Assume the same notations as in §2.3, where the activation to softmax follows a Gaussian  $\mathbf{a} \sim \mathcal{N}(\boldsymbol{\mu}, \mathbf{S})$ .

$$\begin{aligned}
e_k &= \mathbb{E}[f_k] = \int \text{SOFTMAX}(a_k) \mathcal{N}(\mathbf{a}; \boldsymbol{\mu}, \mathbf{S}) d\mathbf{a} \\
&= \int \frac{1}{1 + \sum_{i \neq k} e^{-(a_k - a_i)}} \mathcal{N}(\mathbf{a}; \boldsymbol{\mu}, \mathbf{S}) d\mathbf{a} \\
&= \int \left( 2 - K + \sum_{i \neq k} \frac{1}{\sigma(a_k - a_i)} \right)^{-1} \mathcal{N}(\mathbf{a}; \boldsymbol{\mu}, \mathbf{S}) d\mathbf{a} \\
&\stackrel{\text{integrate}}{\approx} \stackrel{\text{independently}}{\left( 2 - K + \sum_{i \neq k} \frac{1}{\mathbb{E}_{p(a_i, a_k)}[\sigma(a_k - a_i)]} \right)^{-1}} \tag{A.1}
\end{aligned}$$

where ‘‘integrate independently’’ means integrating each term in the summand independently, resulting the expectation to the marginal distribution over the pair  $(a_i, a_k)$ . This approximation is prompted by the mean-field approximation:  $\mathbb{E}[f(x)] \approx f(\mathbb{E}[x])$  for a nonlinear function  $f(\cdot)$ <sup>3</sup>.

Next we plug in the approximation to  $\mathbb{E}[\sigma(\cdot)]$  where  $\sigma(\cdot)$  is the sigmoid function, which states that

$$\int \sigma(x) \mathcal{N}(x; \mu, s^2) dx \approx \sigma\left(\frac{\mu}{\sqrt{1 + \lambda_0 s^2}}\right). \tag{A.2}$$

$\lambda_0$  is a constant and is usually chosen to be  $\pi/8$  or  $3/\pi^2$ . This is a well-known result, see [6]. We further approximate by considering different ways to compute the bivariate expectations in the denominator.

**Mean-Field 0 (mf0)** In the denominator, we ignore the variance of  $a_i$  for  $i \neq k$  and replace  $a_i$  with its mean  $\mu_i$ , and compute the expectation only with respect to  $\alpha_k$ . We arrive at

$$e_k \approx \left( 2 - K + \sum_{i \neq k} \frac{1}{\mathbb{E}_{p(a_k)}[\sigma(a_k - \mu_i)]} \right)^{-1}.$$

Applying eq.(A.2), we have

$$e_k \approx \left( 2 - K + \sum_{i \neq k} \frac{1}{\sigma\left(\frac{\mu_k - \mu_i}{\sqrt{1 + \lambda_0 s_k^2}}\right)} \right)^{-1} = \left( \sum_i \exp\left(-\frac{\mu_k - \mu_i}{\sqrt{1 + \lambda_0 s_k^2}}\right) \right)^{-1}. \tag{A.3}$$

**Mean-Field 1 (mf1)** If we replace  $p(a_i, a_k)$  with the two independent marginals  $p(a_i)p(a_k)$  in the denominator, recognizing  $(a_k - a_i) \sim \mathcal{N}(\mu_k - \mu_i, s_i^2 + s_k^2)$ , we get,

$$e_k \approx \left( 2 - K + \sum_{i \neq k} \frac{1}{\sigma\left(\frac{\mu_k - \mu_i}{\sqrt{1 + \lambda_0 (s_i^2 + s_k^2)}}\right)} \right)^{-1} = \left( \sum_i \exp\left(-\frac{\mu_k - \mu_i}{\sqrt{1 + \lambda_0 (s_i^2 + s_k^2)}}\right) \right)^{-1}. \tag{A.4}$$

<sup>3</sup>Similar to the classical use of mean-field approximation on Ising models, we use the term mean-field approximation to capture the notion that the expectation is computed by considering the weak, pairwise coupling effect from points on the lattice, i.e.,  $a_i$  with  $i \neq k$ .

**Mean-Field 2 (mf2)** Lastly, if we compute eq.(A.1) with a full covariance between  $a_i$  and  $a_k$ , recognizing  $(a_k - a_i) \sim \mathcal{N}(\mu_k - \mu_i, s_i^2 + s_k^2 - 2s_{ik})$ , we get

$$e_k \approx \left( 2 - K + \sum_{i \neq k} \frac{1}{\sigma \left( \frac{\mu_k - \mu_i}{\sqrt{1 + \lambda_0(s_i^2 + s_k^2 - 2s_{ik})}} \right)} \right)^{-1}$$

$$= \left( \sum_i \exp \left( -\frac{\mu_k - \mu_i}{\sqrt{1 + \lambda_0(s_k^2 + s_i^2 - 2s_{ik})}} \right) \right)^{-1}. \quad (\text{A.5})$$

We note that [12] has developed the approximation form eq.(A.5) for computing  $e_k$ , though the author did not use it for uncertainty estimation.

## B Experiments

### B.1 Definitions of evaluation metrics

**NLL** is defined as the KL-divergence between the data distribution and the model’s predictive distribution,

$$\text{NLL} = -\log p(y|x) = -\sum_{c=1}^K y_c \log p(y = c|x) \quad (\text{B.1})$$

where  $y_c$  is the one-hot embedding of the label.

**ECE** measures the discrepancy between the predicted probabilities and the empirical accuracy of a classifier in terms of  $\ell_1$  distance. It is computed as the expected difference between per bucket confidence and per bucket accuracy, where all predictions  $\{p(x_i)\}_{i=1}^N$  are binned into  $S$  buckets such that  $B_s = \{i \in [N] | p(x_i) \in I_s\}$  are predictions falling within the interval  $I_s$ . ECE is defined as,

$$\text{ECE} = \sum_{s=1}^S \frac{|B_s|}{N} |\text{conf}(B_s) - \text{acc}(B_s)|, \quad (\text{B.2})$$

where  $\text{conf}(B_s) = \frac{\sum_{i \in B_s} p(x_i)}{|B_s|}$  and  $\text{acc}(B_s) = \frac{\sum_{i \in B_s} \mathbf{1}[\hat{y}_i = y_i]}{|B_s|}$ .

### B.2 Details of experiments in the main text

Table B.5 provides key hyper-parameters used in training deep neural networks on different datasets.

Table B.5: Hyper-parameters of neural network trainings

Dataset	MNIST	CIFAR-10	CIFAR-100	ImageNet
Architecture	MLP	ResNet20	Densenet-BC-121	ResNet50
Optimizer	Adam	Adam	SGD	SGD
Learning rate	0.001	0.001	0.1	0.1
Learning rate decay	exponential $\times 0.998$	staircase $\times 0.1$ at 80, 120, 160	staircase $\times 0.1$ at 150, 225	staircase $\times 0.1$ at 30, 60, 80
Weight decay	0	$1e^{-4}$	$5e^{-4}$	$1e^{-4}$
Batch size	100	8	128	256
Epochs	100	200	300	90

For mflJ method, we use  $\lambda_0 = \frac{3}{\pi^2}$  in our implementation. For the ENSEMBLE approach, we use  $M = 5$  models on all datasets as in [43]. For RUE, DROPOUT, BNN (VI) and BNN(KFAC), where sampling is applied at inference time, we use  $M = 500$  Monte-Carlo samples on MNIST, and  $M = 50$  on CIFAR-10, CIFAR-100 and ImageNet. We use  $B = 10$  buckets when computing ECE on MNIST, CIFAR-10 and CIFAR-100, and  $B = 15$  on ImageNet.

### B.3 Apply the mean-field approximation to other Gaussian posteriors inference tasks

Table B.6: Uncertainty estimation with SWAG on MNIST

Approx. method	MNIST: in-domain ( $\downarrow$ )	NotMNIST: OOD detection ( $\uparrow$ )					
		$\varepsilon$ (%)	NLL	ECE	Acc. (%)	AU ROC	AU PR (in : out)
sampling $M =$	20	<b>1.55</b>	0.06	0.60	85.78	91.15	<b>91.91</b> : 90.34
	100	<b>1.55</b>	0.06	0.60	<b>88.33</b>	93.19	86.95 : <b>95.72</b>
	500	<b>1.55</b>	0.06	0.60	82.68	88.80	82.51 : 91.23
mean-field ( $M = 0$ )	mf0	1.56	<b>0.05</b>	<b>0.25</b>	87.56	<b>93.26</b>	91.49 : 93.96
	mf1	<b>1.55</b>	0.05	0.46	85.28	90.68	85.15 : 92.39
	mf2	1.55	0.05	0.51	82.18	87.40	78.12 : 90.69

The mean-field approximation is interesting in its own right. In particular, it can be applied to approximate any Gaussian-softmax integral. In this section, we apply it to the SWA-Gaussian posterior (SWAG) [33], whose covariance is a low-rank matrix plus a diagonal matrix derived from the SGD iterates. We tune the ensemble and activation temperatures with SWAG to perform uncertainty tasks on MNIST, and the results are reported in Table B.6. We ran SWAG on the softmax layer for 50 epochs, and collect models along the trajectory to form the posterior.

We use the default values for other hyper-parameters, like SWAG learning rate and the rank of the low-rank component, as the main objective here is to combine the mean-field approximation with different Gaussian posteriors. As we can see from Table B.6, SWAG, when using sampling for approximate inference, have a variance larger than expected<sup>4</sup>. Nonetheless, within the variance, using the mean-field approximation instead of sampling performs similarly. The notable exception is in-domain tasks where the mean-field approximation consistently outperforms sampling.

This suggests that the mean-field approximations can work with other Gaussian distributions as a replacement for sampling to reduce the computation cost.

Table B.7: Uncertainty estimation on CIFAR-10

Method	CIFAR-10 in-domain ( $\downarrow$ )			LSUN: OOD detection ( $\uparrow$ )			SVHN: OOD detection ( $\uparrow$ )		
	$\varepsilon$ (%)	NLL	ECE (%)	Acc.	AU ROC	AU PR (in/out)	Acc.	AU ROC	AU PR (in : out)
MLE	8.81	0.30	3.59	85.0	91.3	93.8 : 87.8	86.3	90.7	89.5 : 92.6
T. SCALE	8.81	0.26	<b>0.52</b>	89.0	95.3	96.5 : 93.4	88.9	94.0	92.7 : 95.0
ENSEMBLE	<b>6.66</b>	<b>0.20</b>	1.37	88.0	94.4	95.9 : 92.1	88.7	93.4	92.4 : 94.8
RUE	8.71	0.28	1.87	85.0	91.3	93.8 : 87.8	86.3	90.7	89.5 : 92.6
DROPOUT	8.83	0.26	0.58	81.8	88.6	91.7 : 84.3	86.0	91.6	90.1 : 94.0
BNN VI	11.09	0.33	1.57	79.9	87.3	90.5 : 83.3	85.7	91.4	89.5 : 93.9
BNN LL-VI	8.94	0.33	4.15	84.6	91.0	93.5 : 87.2	87.8	93.3	91.7 : 95.4
BNN(KFAC)	8.75	0.29	3.45	85.0	91.3	93.8 : 87.8	86.3	90.7	89.5 : 92.6
mfI	8.81	0.26	0.56	<b>91.0</b>	<b>96.4</b>	<b>97.4 : 94.8</b>	<b>89.7</b>	<b>94.6</b>	<b>93.3 : 95.3</b>

Table B.8: Out of Distribution Detection on CIFAR-100

Method	SVHN: OOD detection ( $\uparrow$ )		
	Acc.	AU ROC	AU PR (in : out)
MLE	73.90	80.69	74.03 : 86.93
T. scaling	76.94	83.43	77.53 : 88.11
Ensemble	75.99	83.48	77.75 : 88.85
RUE	73.90	80.69	74.03 : 86.93
Dropout	74.13	81.87	75.78 : 88.07
BNN LL-VI	71.87	79.55	72.08 : 87.27
BNN(KFAC)	74.13	80.97	74.46 : 87.06
mfI	<b>81.38</b>	<b>88.04</b>	<b>84.59 : 91.23</b>

<sup>4</sup>In particular, the variance is higher than the variance in the sampling results of the infinitesimal jackknife, cf. Table 2 in the main text.

Table B.9: NLLs and RMSEs of different methods on regression benchmark datasets.

Metrics	Dataset	ENSEMBLE [28] <sup>†</sup>	RUE [42]	DROPOUT [16] <sup>†</sup>	BNN (PBP) [22] <sup>†</sup>	BNN (KFAC) [41]	mflJ
NLL (↓)	Housing	<b>2.41 ± 0.25</b>	2.69 ± 0.44	2.46 ± 0.06	2.57 ± 0.09	2.74 ± 0.46	<b>2.66 ± 0.39</b>
	Concrete	3.06 ± 0.18	3.21 ± 0.14	<b>3.04 ± 0.02</b>	3.16 ± 0.02	3.25 ± 0.18	3.15 ± 0.09
	Energy	<b>1.38 ± 0.22</b>	1.48 ± 0.35	1.99 ± 0.02	2.04 ± 0.02	1.48 ± 0.35	<b>1.47 ± 0.35</b>
	Kin8nm	<b>-1.20 ± 0.02</b>	-1.13 ± 0.03	-0.95 ± 0.01	-0.90 ± 0.01	-1.14 ± 0.03	-1.15 ± 0.02
	Naval	-5.63 ± 0.05	<b>-6.00 ± 0.22</b>	-3.80 ± 0.01	-3.73 ± 0.01	-5.99 ± 0.22	<b>-5.99 ± 0.22</b>
	Power	<b>2.79 ± 0.04</b>	2.86 ± 0.04	2.80 ± 0.01	2.84 ± 0.01	2.86 ± 0.04	2.86 ± 0.04
	Wine	<b>0.94 ± 0.12</b>	0.99 ± 0.06	0.93 ± 0.01	0.97 ± 0.01	0.99 ± 0.08	<b>0.99 ± 0.07</b>
	Yacht	1.18 ± 0.21	<b>1.14 ± 0.42</b>	1.55 ± 0.03	1.63 ± 0.02	1.66 ± 0.88	<b>1.18 ± 0.53</b>
RMSE (↓)	Housing	3.28 ± 1.00	3.34 ± 0.94	<b>2.97 ± 0.19</b>	3.01 ± 0.18	3.42 ± 1.09	3.24 ± 0.93
	Concrete	6.03 ± 0.58	5.67 ± 0.65	<b>5.23 ± 0.12</b>	5.67 ± 0.09	5.65 ± 0.63	5.60 ± 0.61
	Energy	2.09 ± 0.29	1.09 ± 0.35	1.66 ± 0.04	1.80 ± 0.05	1.08 ± 0.35	<b>1.08 ± 0.35</b>
	Kin8nm	0.09 ± 0.00	<b>0.08 ± 0.00</b>	0.10 ± 0.00	0.10 ± 0.00	0.08 ± 0.00	<b>0.08 ± 0.00</b>
	Naval	<b>0.00 ± 0.00</b>	0.00 ± 0.00	0.01 ± 0.00	0.01 ± 0.00	0.00 ± 0.00	<b>0.00 ± 0.00</b>
	Power	4.11 ± 0.17	4.21 ± 0.15	<b>4.02 ± 0.04</b>	4.12 ± 0.03	4.21 ± 0.15	4.21 ± 0.15
	Wine	0.64 ± 0.04	0.65 ± 0.04	<b>0.62 ± 0.01</b>	0.64 ± 0.01	0.65 ± 0.04	0.65 ± 0.04
	Yacht	1.58 ± 0.48	0.82 ± 0.26	1.11 ± 0.09	1.02 ± 0.05	1.19 ± 1.08	<b>0.80 ± 0.25</b>

<sup>†</sup>: numbers are cited from the original paper.

#### B.4 More results on CIFAR-10 and CIFAR-100

Tables B.7 and B.8 supplement the main text with additional experimental results on the CIFAR-10 dataset with both in-domain and out-of-distribution detection tasks, and on the CIFAR-100 with out-of-distribution detection using the SVHN dataset. BNN LL-VI refers to stochastic variational inference on the last layer only.

The results support the same observations in the main text: mflJ performs similar to other approaches on in-domain tasks, but noticeably outperforms them on out-of-distribution detection.

#### B.5 Regression experiments

We conduct real-world regression experiments on UCI datasets. We follow the experimental setup in [16, 22, 28], where each dataset is split into 20 train-test folds randomly, and the average results with the standard deviation are reported. We use the same architecture as previous works, with 1 hidden layer of 50 ReLU units. Since in regression tasks the output distribution can be compute analytically, we don't use the mean-field approximation in these experiments. Nevertheless, we still refer to our method as mflJ to be consistent with other datasets.

For mflJ approach, we use the pseudo-ensemble Gaussian distribution of *the last layer* parameters to compute a Gaussian distribution of the network output, *i.e.*  $a \sim \mathcal{N}(\mu(x), s^2(x))$  as eq. (9) in the main text. We also estimate the variance of the observation noise  $\epsilon^2$  from the residuals on the training set [42]. Therefore, the predictive distribution of  $f(x)$  is given by  $\mathcal{N}(\mu(x), s^2(x) + \epsilon^2)$ . We can compute the negative log likelihood (NLL) as,

$$\text{NLL} = -\log p(y|x) = \frac{1}{2} \left( \log(s^2(x) + \epsilon^2) + \frac{(y - \mu(x))^2}{s^2(x) + \epsilon^2} + \log(2\pi) \right).$$

We tune ensemble temperature on the heldout sets, and fix the activation temperature to be 1.

For sampling-based methods, RUE and KFAC, the NLL from  $M$  prediction sample  $f_1(x), \dots, f_M(x)$  can be computed as,

$$\text{NLL} = -\log p(y|x) = \frac{1}{2} \left( \log(\bar{s}_m^2 + \epsilon^2) + \frac{(y - \bar{\mu}_m)^2}{\bar{s}_m^2 + \epsilon^2} + \log(2\pi) \right)$$

where  $\bar{\mu}_m = \frac{1}{M} \sum_m f_m(x)$  is the mean of prediction samples, and  $\bar{s}_m^2 = \frac{1}{M} \sum_m (f_m(x) - \bar{\mu}_m)^2$  is the variance of prediction samples. The sampling is conducted on all network layers in both RUE and KFAC.

**Results** We report the NLL and RMSE on the test set in Table B.9 and compare with other approaches. RUE and BNN(KFAC) use  $M = 50$  samples and the ENSEMBLE method has  $M = 5$  models in the ensemble. We achieve similar or better performances than RUE and KFAC without



the computation cost of explicit sampling. Compared to DROPOUT and ENSEMBLE, which are the state-of-the-art methods on these datasets, we also achieve competitive results. We highlight the best performing method on each dataset, and mflJ when its result is within one std from the best method.

### B.6 More results on comparing all layers versus just the last layer.

We conduct an experiment similar to the top portion of Table 2 in the main text, to study the effect of restricting the parameter uncertainty to the last layer only. We use NotMNIST as the in-domain dataset and treat MNIST as the out-of-distribution dataset. We use a two-layer MLP with 256 ReLU hidden units. Table B.10 supports the same observation as in the main text: restricting to the last layer improves on OOD task while it does not have significant negative impact on the in-domain tasks.

Table B.10: Performance of infinitesimal jackknife pseudo-ensemble distribution on NotMNIST comparing all layers versus just the last layer

which layer(s)	approx. method		NotMNIST: in-domain ( $\downarrow$ )			MNIST: OOD detection ( $\uparrow$ )		
			$\varepsilon$ (%)	NLL	ECE	Acc. (%)	AU ROC	AU PR (in : out)
all	sampling	500	3.18	0.12	0.43	90.73	95.14	97.09 : 89.78
last	$M =$	500	3.18	0.12	0.43	<b>92.26</b>	<b>96.23</b>	<b>97.82 : 92.06</b>